

Catchment basin versus Mountain range tessellations from DTMs for islands: Lesvos, Kerguelen, Crete, Cyprus, New-Caledonia, Formosa and Sri Lanka

Christian Depraetere¹, Serge Riazanoff²

¹ Institut de Recherche pour le Développement (IRD), Maison de la Télédétection, Montpellier 34000, France

² VisioTerra, Scientific consulting for earth observation, rue Albert Einstein, 77420 Champs-sur-Marne, France
Email: corresponding author christian.depraetere@ird.fr

Abstract.

The aim is to compare the geomorphometric signatures of catchment basins (using Steepest Descent lines converging to Outlets, SDO) and mountain ranges ('massifs', using Steepest Ascent lines Toward Summits, SATS) on a set of islands in various topographical, geological and morphoclimatic settings: Lesvos (1656 km², 39.51°N, max elevation 903 meters), Kerguelen (6761 km², 49.19°S, 1792 m), Crete (8325 km², 35.31°N, 2442 m), Cyprus (9230 km², 35.13°N, 1971 m), 4205 m), New-Caledonia (16 469 km², 21.24°S, 1621 m), Formosa (35 901 km², 23.6°N, 3917 m), and Sri Lanka (66 375 km², 7.87°N, 2518 m. For comparability, the same SRTM 3 arc second DTM is used. While the SDO basin tessellation depends mostly on hydrological processes, the dual fragmentations given by the SATS are conversely more related to the lithology and the tectonics of mountainous areas. The main hypothesis is that there are relationships between environmental factors and pattern signatures for both catchment basins and mountain ranges.

The tessellation of catchment basins uses the D8 steepest descent method available in most GIS toolboxes. On the other hand, our *ad hoc* stepwise algorithm (MAPAM) delineates elementary hills up to the major mountain ranges associated with highest summits. The outcome of merging SDO and SATS is a combined tessellation in which tiles are landform units (LU2s) collecting water from the same slope within the same catchment and collected by the same section of river (thalweg) between two confluences. The statistical textural properties of the tiles are analyzed for both SDO and SATS tessellations and the resulting LU2s combined patterns on the seven islands are compared using the area-number method also called "Korčák Number-Area law". The size distributions are fitted with the power law functions $N=\alpha \cdot A^{-\beta}$. The parameter β varies with geological context and morphogenic climatic factors.

Coupled with other geostatistical approaches for land or bathymetric surface analysis (i.e. variograms, geomorphometry, etc.), this combined SDO and SATS tessellation contributes to innovative semi-automatic survey and mapping methods for a wide range of environmental applications, for instance topographical habitats, distributed hydrological modeling, geomorphologic risk assessment and transportation planning optimization.

Keywords: DTM, steepest descent and ascent, tessellation, Korcak exponent, islands, catchments, mountains.

1 Introduction

DTM algorithms contribute to deciphering the terrestrial landform patterns resulting from complex and entangled geomorphologic processes. Several pioneering researches on the topology of closed contour line maps date from the mid-nineteenth century: Reech (1858, [1]), Cayley (1859, [2]) and especially Maxwell (1870, [3]), considered as the "first quantitative geomorphologist" [4]. Our work with GIS tools builds upon their ideas. By analogy with physics, the following research deals with properties of the "vector field" as the codomain of the "scalar field" of the topography given by DTM. Two kinds of topographical "footprints" are hereby extracted from the DTM (Figure 1A) by specific algorithms; the "downprint" (Figure 1B) referring to a tessellation of catchment basins related to outlets along the shores (steepest descent to lowest points) and the "upprint" (Figure 1C) as a pattern of converging steepest ascent lines toward highest points such as small bumps, hill tops or mountain summits, with embedded magnitudes [5]. These landform units are defined as "massifs" (as "anti-catchments" related to high points) and are complementary to catchments. Both types can be labelled "land units".

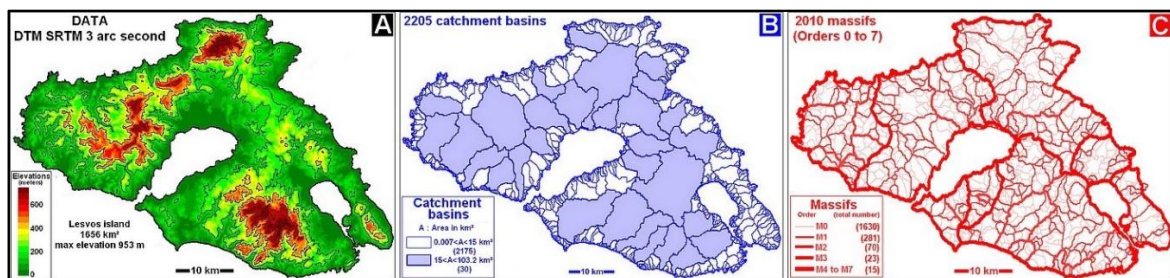


Figure 1 Altitudes from DTM 3 arc second (A); tessellations of catchment basins (B) and massifs (C) on Lesvos island

The tessellations will be applied to 7 islands of different shapes, with areas ranging from 1600 to 63 000 km², located in various morphoclimatic and geologic environments: Mediterranean (Lesvos, Crete and Cyprus), tropical (New-Caledonia and Formosa), equatorial (Sri Lanka) and subpolar (Kerguelen). For statistical analysis the Korčak number-area law (or "rule") and the Korcak exponent are used to quantify the fragmentation patterns.

2 Data and Methods

Data: the results are calculated from the same SRTM 3 arc second DTM for all 7 islands, with a resolution of about 100 meters and a vertical accuracy of the order of few meters, suitable for hilly and mountainous areas but not for gently undulated plains. A DTM with better landform rendering (i.e. Lidar) would give the same tessellation on large landform units but more details on flattish bumpy areas.

Methods for catchment basin and massif tessellations: geoscientists are familiar with the D8 method calculating Steepest Descent lines converging to Outlets (SDO) that allows the extraction of catchment basins and their watersheds shaping the topographic "downprint" of a region (Figure 1B). Conversely, the delineation of Steepest Ascent lines Toward Summits (SATS) are not often compute despite being the dual graph of SDO and providing the complementary "upprint" of the topography (Figure 1C): the landform units correspond to bumps, hills and mountains. These upprint units will be defined as "massifs" whatever their size and relief amplitude. The ad hoc stepwise algorithm MAPAM (Massifs PARTitioning Method [6] and [7]) for massif tessellation applies the same D8 method [8] on the inverted DTM with elevation turned upside down, as a first step (Initial or elementary massifs of order 0). At further steps, the massifs are merged step by step (Massifs of order 1, 2, and so on) according to the pathways through saddle points presenting the most amplitude from surrounding high points. At the final stage, all the massifs are merge into one unit associated with the highest summit. As illustrated by the Rasemann's diagram of Figure 2, it is worth noticing that the SATS are not an inversion of SDO which is somehow counter intuitive at first though.

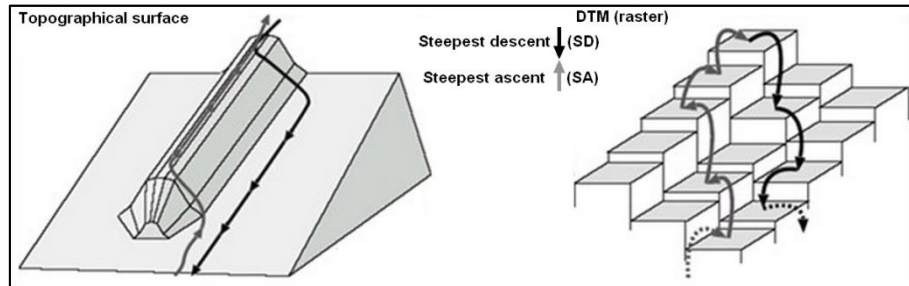


Figure 2 Slope lines derived up (SA) and down (SD) the slope take different courses when plan curvature occurs (After from [9])

(Note that the MAPAM algorithm was conceived in 2004 [6] without knowing that James Clerk Maxwell had the same idea in 1870 [3]: according to him, the secondary summits around a main summit could be topologically considered as vertical "saddle points" - which is exactly what MAPAM is doing.)

The properties of size (Area A) distributions (Number N) of both catchments and massifs are summarized by the Korčák Number (N) - Area (A) empirical law [page 70 of [10]]

$$N(A > A_0) = \alpha \cdot A_0^{-\beta}, \text{ with } N \text{ the number of objects with area } A \text{ greater than area } A_0 \quad (1)$$

By convention, the parameter β is called Korčák's exponent of the power function fitted to the size distribution. This exponent is compared for the tessellation patterns of catchments and massifs on the 7 islands. For instance on Lesbos island (Figure 3), the parameter β is equal to 0.623 for catchments and 0.839 for massifs, with the SRTM 3 arc second DTM. For this island, large catchments with $A > 15 \text{ km}^2$ do not conform to the distribution functions and small catchments ($A < 0.1 \text{ km}^2$) and massifs ($A < 1 \text{ km}^2$) are under-sampled. It has to be mentioned that the Korčák exponent is a non-fractal descriptor for topographic patchiness and geographic features [11] [12] contrariwise with one of Mandelbrot's hypothesis [13].

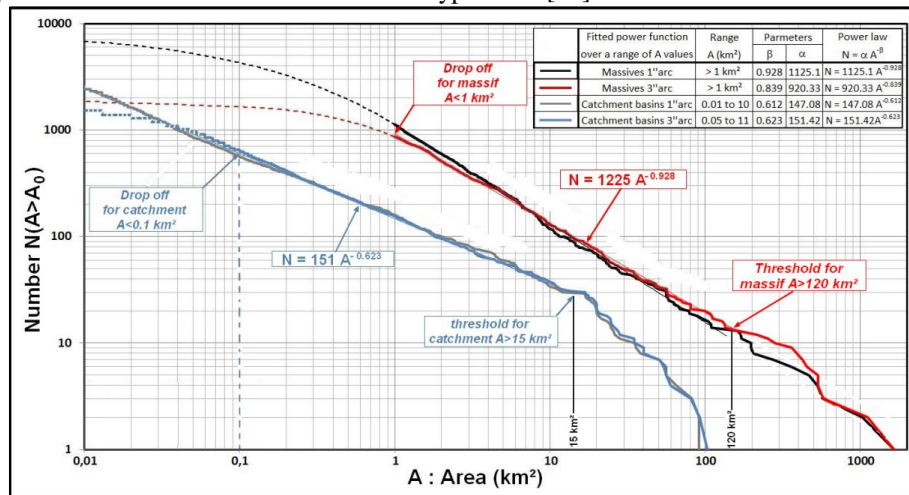


Figure 3 Korčák number-area laws for catchment basins and massifs on Lesbos island (NB: the results shows minor discrepancies between the 1arc and 3 arc second SRTM DTMs)

3 Results: The number-area law and the Korcak exponents on the 7 islands

Figure 4 shows that according to the number-area method the size distributions of catchments and massifs (with $A > 1 \text{ km}^2$ for both) are quite similar despite the differences of size, shape and environmental contexts of each island. The main points about the fitted power functions (See (1)) are as follow:

- The parameter α is the number N of land units with $A > 1 \text{ km}^2$ (depending mostly on the island size);
- The parameter β (or Korcak exponent) is the “slope” of the size distribution on a log-log graph and reflects the homogeneity of patchiness over a class of areas (Figure 4A): i.e. on Lesvos, $\beta = 0.62$ for the catchments with $1 < A < 15 \text{ km}^2$, $\beta = 0.93$ for the massifs with $1 < A < 120 \text{ km}^2$;
- The size distributions are “steeper” for massifs ($0.86 < \beta < 0.93$) compared to catchments ($0.45 < \beta < 0.75$). Fits are best for land units $1 < A < 100 \text{ km}^2$;
- Above a threshold value of A , the largest land units depart from the distribution functions calibrated on smaller land units: i.e. on Lesvos, for large catchments ($A > 15 \text{ km}^2$), and massifs ($A > 120 \text{ km}^2$).

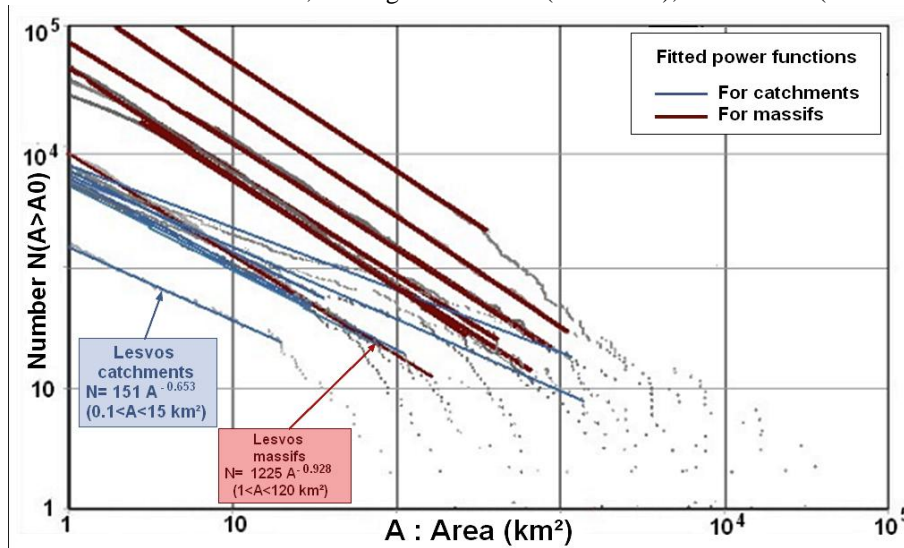


Figure 4 Size (Area) distribution properties for catchments and massifs with the Korcak method for the 7 islands.

4 Discussion

For comparison, **Figure 5** plots the Korcak exponents combining both catchments (β_c) and massifs (β_m) from the empirical results of Figure 3A. Depending on various factors, each island has a different (β_c , β_m) “signature”. The sharpest contrast for catchment signatures is between Sri Lanka ($\beta_c = 0.45$, equatorial, oval shape) and Kerguelen ($\beta_c = 0.75$, sub polar, coastline with fjords). The massif signatures tend to be similar with an average value $\beta_m = 0.89$, except for lower values for Crete ($\beta_m = 0.86$, Mediterranean), Kerguelen ($\beta_m = 0.86$) and higher for Lesvos ($\beta_m = 0.93$, Mediterranean).

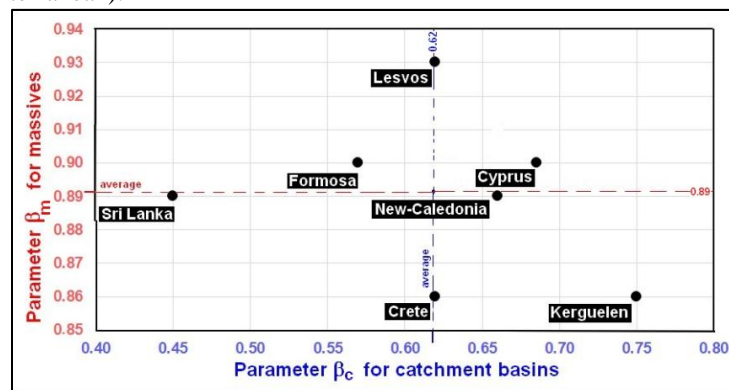


Figure 5 Combined (β_c, β_m) signatures of catchments and massifs according to the Korcak exponents

These empirical findings from a limited set of 7 islands cannot assume to be representative of all land patterns but they give insights to more theoretical works. For instance, Figure 6 could be a theoretical prototype for the most frequent landform pattern signatures (β_c, β_m) characterizing islands. It could apply also to mountain ranges but not to non-islands where border effects cause distortions. It is not suitable for karstic or endorheic regions.

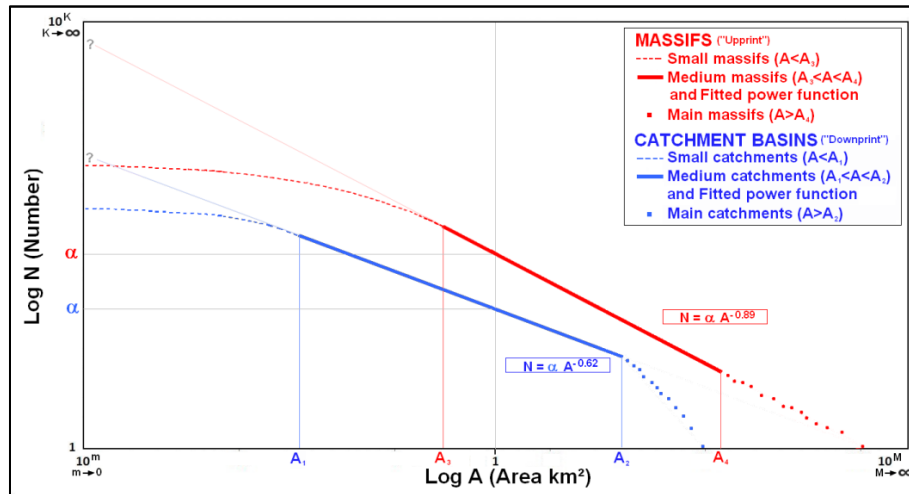


Figure 6 Adimensional prototype of landform patterns (Signature (β_c, β_m)) on islands from **Figure 5**.

It is worth noting that the embedded hierarchy of massifs from order 0 onward is similar to the notion of sub-catchments within a catchment: most often, the main summit of a large massif (A mountain range of high order) is surround by several secondary summits (Mountains of medium order). In their turn, these minor peaks may be flanked by smaller elementary massifs (hills and bumps of order 0). Similarly, the boundaries between massifs correspond to the notion of watersheds or water divides. These “anti-watershed” lines follow the thalwegs and the pathways connecting them through saddle points. This crisscrossing of lines for instance on Lesbos island (Figure 1C) tends to be associated with faults and weak rocks and...transportation networks.

5 Conclusions

- As a dual pattern of catchment basin tessellations, the massif patches give complementary information on the relationships of hydrological processes with geology and tectonics.
- Topographical downprint and upprint power functions are relevant to estimate size distributions of catchment basins and massifs on islands.
- This quantitative approach to landforms should be combine with other geomorphometric methods such as variograms, hypsometric curves, geomorphological hydrographs, etc.
- The empirical Korcak number-area rule is valuable for a theoretical approach to these landforms.
- Beyond GIS, geomorphological mapping and theoretical research, the methods are relevant for applications in several scientific domains such as hydrology, geomorphology, potamology and structural geology but also transportation operational research and geoarchaeology.

References

- Reech, M.: Propriété générale des surfaces fermées. Ecole Polytech. Jour. Paris, 1858, v. 37, p. 169–178 (1858).
- Cayley, A.: On contour lines and slope lines. Phil. Mag., 1859, v. 18, p. 264–268 (1859).

3. Maxwell, J. C.: On hills and dales. *Phil. Mag.*, 1870, v. 40, p. 421–427 (1870)
4. Cockbain, A. E.: James Clerk Maxwell, the first quantitative geomorphologist?. *Math. Geol.*, 1980, v. 12, p. 615–616.
5. Depraetere C., Riazanoff S.: Downprint and upprint of landforms from DEM: the case of the volcanic Acores islands. 10th International Conference of the International Association of Geomorphologists (IAG), Coimbra, Portugal, 12-16 September 2022. (2022). <https://meetingorganizer.copernicus.org/ICG2022/ICG2022-631.html>
6. Depraetere C., Riazanoff S.: The new Digital Elevation Model data set from the Shuttle Radar Topography Mission: hydrogeomorphological applications in the Ohrid region. Conference BALWOIS, Ohrid, Northern Macedonia, 25-29 May 2004 (2004). https://igm.univ-mlv.fr/~riazano/publications/20040525_BALWOIS_Conference.pdf
7. Depraetere, C.: Introduction à l'hydrogéomorphométrie : études des relations entre le modelé des formes de terrain et les processus hydrologiques dans des contextes insulaires. Habilitation à diriger des recherches (HDR), 2013, Université Paris-Diderot PVI. (2013). https://www.espace-dev.fr/wp-content/uploads/2020/11/HDR_Christian_Depraetere_Document_Inedit_Novembre_2013_Part1.pdf
8. Shin, S., Paik, K.: An improved method for single flow direction calculation in grid digital elevation models. *Hydrol. Proc.* 31 (8), 1650-1661. (2017) <https://doi.org/10.1002/hyp.11135>
9. Rasemann, S.: "Geomorphometrische Struktur eines mesoskaligen alpinen Geosystems". Dissertation zur Erlangung des Doktorgrades (PhD), Friedrich-Wilhelms-Universität, Bonn 2003, 339 pages. (2003). http://tolu.giub.uni-bonn.de/grk/download/phd_rasemann.pdf
10. Korčák, J.: Deux types fondamentaux de distribution statistique, *Bull. Inst. Int. de Statistique* III: 295-299. (1940).
11. Imre, A.R., Novotný, J., Rocchini, D.: The Korcak-exponent: A non-fractal descriptor for landscape patchiness. *Ecological complexity*. 12. 70-74. <https://doi.org/10.1016/j.ecocom.2012.10.001> (2012).
12. Imre, A., Novotný, J.: Fractals and the Korcak-law: a history and a correction. *EPJ H* 41, 69–91 2016 (2016). <https://doi.org/10.1140/epjh/e2016-60039-8>
13. Mandelbrot, B.B.: Stochastic models for the Earth's relief, shape and fractal dimension of coastlines, and number-area rule for islands, *Proc. Natl. Acad. Sci. USA* 72: 3825-3838. (1975)